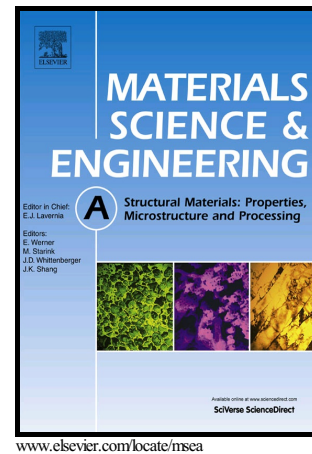


Author's Accepted Manuscript

Microstructural evolution and superplasticity in an Mg–Gd–Y–Zr alloy after processing by different SPD techniques

R. Alizadeh, R. Mahmudi, P.H.R. Pereira, Y. Huang, T.G. Langdon



PII: S0921-5093(16)31444-7
DOI: <http://dx.doi.org/10.1016/j.msea.2016.11.080>
Reference: MSA34406

To appear in: *Materials Science & Engineering A*

Received date: 8 September 2016
Revised date: 22 November 2016
Accepted date: 23 November 2016

Cite this article as: R. Alizadeh, R. Mahmudi, P.H.R. Pereira, Y. Huang and T.G. Langdon, Microstructural evolution and superplasticity in an Mg–Gd–Y–Zr alloy after processing by different SPD techniques, *Materials Science & Engineering A*, <http://dx.doi.org/10.1016/j.msea.2016.11.080>

This is a PDF file of an unedited manuscript that has been accepted for publication. As a service to our customers we are providing this early version of the manuscript. The manuscript will undergo copyediting, typesetting, and a review of the resulting galley proof before it is published in its final citable form. Please note that during the production process errors may be discovered which could affect the content, and all legal disclaimers that apply to the journal pertain

Microstructural evolution and superplasticity in an Mg–Gd–Y–Zr alloy after processing by different SPD techniques

R. Alizadeh^a, R. Mahmudi^{a,*}, P.H.R. Pereira^b, Y. Huang^b, T.G. Langdon^b

^a*School of Metallurgical and Materials Engineering, College of Engineering, University of Tehran, Tehran, Iran.*

^b*Materials Research Group, Faculty of Engineering and the Environment, University of Southampton, Southampton SO17 1BJ, U.K.*

*Corresponding author: Phone: +98 21 8208 4137, Fax: +98 21 8800 6076. e-mail: mahmudi@ut.ac.ir

Abstract

Mg–Gd–Y–Zr alloys have attracted much attention recently due to their ability to exhibit stable fine-grained microstructures and their potential superplastic behavior. However, the microstructure and superplasticity of these alloys processed by severe plastic deformation (SPD) methods remain less understood. In this work, the microstructure and superplastic behavior of an Mg–5Gd–4Y–0.4Zr (GW54) alloy were investigated after processing using extrusion and the SPD processes of equal-channel angular pressing (ECAP) and high-pressure torsion (HPT). Microstructural characterization by transmission electron microscopy and electron backscattered diffraction showed that nano-sized grains of $\sim 72 \pm 5$ nm were obtained after 8 HPT turns whereas the grain sizes were about $\sim 4.6 \pm 0.2$ and $\sim 2.2 \pm 0.2$ μm after extrusion and 4 ECAP passes, respectively. Shear punch tests revealed that the optimum temperature for superplasticity is 623 K for the HPT samples and 723 K for the ECAP and extrusion samples, at which the strain rate sensitivity were measured as about 0.42 ± 0.05 , 0.46 ± 0.05 and 0.50 ± 0.05 for the extrusion, ECAP and HPT samples, respectively, and the corresponding activation energies were about 117, 101 and 110 ± 5 kJ/mol for these three processing conditions. These results suggest that grain boundary sliding controlled by grain boundary diffusion is the dominant mechanism of deformation at the optimum temperatures for superplastic flow.

Keywords:

ECAP; HPT; Mg–Gd–Y–Zr alloys; Nano-grained; Shear punch test; Superplasticity

1. Introduction

Low density, good castability, high specific strength and stiffness, and reasonable cost make magnesium alloys attractive for aerospace and automotive applications. Despite these advantages, poor formability at low temperatures is one of the most important limitations of Mg alloys. This disadvantage arises from the limited slip systems in the hexagonal close-packed (hcp) structure [1]. In order to overcome this limitation, attempts have been made to enhance their formability through grain refinement and the use of superplastic forming which will permit the fabrication of lightweight structural components having complex shapes [2–5]. Severe plastic deformation processes (SPD), with the capability of imposing large amounts of strain, have been used extensively for grain refinement and thus improving the formability of Mg alloys. For SPD processing, equal-channel angular pressing (ECAP) and high-pressure torsion (HPT) are among the most conventional and effective methods used to achieve grain refinement and superplasticity in different Mg alloys.

Concerning the grain refinement efficiency of different SPD methods, although there have been many investigations in the literature on the superplasticity of different Mg alloys after processing by ECAP or HPT, there are only limited comparisons between the grain refinement efficiency of the different methods. While such a comparison was made previously [6] between HPT, ECAP, accumulative roll bonding (ARB) and ball milling (BM) based on data for Ni, Fe, and Al materials, there has been no comparison for Mg or Mg alloys. In addition, the resultant effects of grain refinement on the superplastic behavior of these materials are not available. A comparison of the grain sizes obtained by ECAP and HPT is given in Table 1 [7–9] for some Cu and Al alloys and it is readily apparent that the grain sizes produced by HPT are much smaller than for ECAP. This difference is due primarily to the much higher strains attained in HPT processing where the ability to achieve smaller grain sizes in HPT was demonstrated in early

experiments [10,11] and, in addition, it was shown more recently that, by comparison with ECAP, HPT produces a higher fraction of grain boundaries having high angles of misorientation [12].

The most important problem of fine-grained Mg alloys produced by SPD methods is the occurrence of microstructural instability at high temperatures. Accordingly, attempts have been made to improve their thermal stability through the addition of different alloying elements. It was reported that the addition of gadolinium (Gd) and other rare earth (RE) elements can lead to a remarkable improvement in the thermal stability of microstructure and mechanical properties at high temperatures due to solution hardening and precipitation strengthening [13,14]. Accordingly, there are many investigations reporting superplasticity in fine grained Mg–Gd alloys with average grain sizes in the range of 1–10 μm processed by extrusion [15–18], friction stir processing (FSP) [19,20] and rolling [21,22]. However, only limited reports are available to date documenting superplasticity in these alloys after processing by ECAP [23,24] or HPT [25].

The strain rate sensitivity (SRS) of materials is a characteristic property of superplastic materials and it can be obtained through localized methods or by conducting conventional tensile testing. Shear punch testing (SPT) is an example of a localized method that introduced recently as an appropriate technique for measuring the SRS in different materials processed by SPD and a summary of the results available to date was given in an earlier report [25]. It should be noted that the validity of the SPT-tensile correlation was demonstrated several years ago [26]. The advantages of studying superplasticity by SPT was described earlier [27] and it includes the requirement for using only very small amounts of material as is readily produced using HPT processing. Thus, SPT is used exclusively in this work to investigate superplasticity.

Although the main features and effects of ECAP and HPT on the microstructure and superplasticity of Mg–Gd–Y–Zr alloys was discussed in earlier publications, a clear comparison between ECAP and HPT cannot be made based on these published data, since they were obtained for different alloys having different concentrations of Gd and Y (for example, the ECAP and HPT were performed on GW50 [24] and GW94 [25] alloys, respectively). This is because the Gd and Y elements can affect the grain size of Mg alloys and this is beyond the scope of the present paper. Therefore, the overall aim of this research was to investigate and compare the microstructural evolution and superplasticity in an Mg–Gd–Y–Zr alloy after processing by extrusion or by extrusion followed by either ECAP or HPT. It has to be mentioned that the optimum ECAP and HPT temperatures and strains were chosen so as to achieve the highest degree of grain refinement which can be obtained by each processing method, based on our earlier experiments on Mg–Gd–Zr [24] and Mg–Gd–Y–Zr alloys [25].

2. Experimental material and procedures

An alloy of Mg–5 wt% Gd–4 wt% Y–0.4 wt% Zr was prepared from high purity Mg, Mg–30Gd, Mg–30Y and Mg–30Zr master alloys by melting in an electric furnace under a covering flux. Tilt-casting was used to minimize casting defects and any melt turbulence. The molten material was poured into a steel die preheated to 573 K and then extrusion was conducted at 673 K using two extrusion ratios of 19:1 to a diameter of 10 mm for HPT samples or 8:1 to square cross-section of $13 \times 13 \text{ mm}^2$ for ECAP samples.

Thin sliced samples with thicknesses of about 1.2 mm were cut from the round extruded bars perpendicular to the extrusion direction using electro-discharge machining (EDM). Both sides of these disks were carefully polished with abrasive papers to prepare a series of samples having thicknesses of about 0.80 mm. The HPT processing was performed under quasi-

constrained conditions [28] using an HPT facility with a rotating lower anvil. All processing was conducted at ambient temperature under an applied pressure, P , of 6.0 GPa. Torsional straining was applied by rotating the lower anvil at a constant speed of 1 rpm through total numbers, N , of 8 revolutions. No damage or cracking was observed after processing by HPT. The ECAP processing was conducted at 623 K using route B_C where each billet is rotated longitudinally by 90° in the same sense between passes [29]. The ECAP die contained a die angle of 90° so that each pass imposed a strain of ~ 1 [30] and the processing was conducted through a total of 4 passes.

A Hitachi S-3400N variable pressure scanning electron microscope (SEM) and an FEI Tecnai G2 20 S-TWIN scanning transmission electron microscope (TEM) with maximum operating voltages of 200 kV were used to study the microstructures of the samples after different deformation conditions. The samples for SEM were etched with an acetic-picral solution. The TEM samples were prepared by ion beam milling (IBM). After grinding these samples to $\sim 100 \mu\text{m}$ thickness, their thicknesses were further reduced to $\sim 20 \mu\text{m}$ with a dimpler machine and the TEM samples were finally prepared by IBM using a milling angle of 12° with a voltage of 4 kV. Electron backscattered diffraction (EBSD) was used to study the orientation maps. The specimen preparation for EBSD involved grinding by SiC paper and diamond paste polishing followed by vibratory polishing with an alcohol-based alumina.

The occurrence of superplasticity was evaluated using SPT using an approach described earlier [31]. The HPT discs and thin slices of the material with thicknesses of $\sim 0.9 \text{ mm}$ cut from the extruded and ECAP bars perpendicular to the extrusion direction were ground to thicknesses of $\sim 0.6 \text{ mm}$. The SPT was performed in the temperature range of 573–673 K for the HPT samples and 623–773 K for the extruded and ECAP samples, using temperature intervals of 50 K

and shear strain rates in the range from 6.5×10^{-3} to $1.3 \times 10^{-1} \text{ s}^{-1}$. The tests were performed using a screw-driven MTS testing system equipped with a three-zone split furnace. A shear punch fixture with a 2.96 mm diameter flat cylindrical punch and 3.04 mm diameter receiving hole was used for SPT. The load, F , was measured automatically as a function of the punch displacement and the data were recorded by appropriate software to determine the shear stress, τ , on the tested material using the relationship [32]

$$\tau = \frac{F}{\pi D t} \quad (1)$$

where t is the specimen thickness and D is the average of the punch and die hole diameters. The SPT curves were then plotted as shear stress against normalized punch displacement.

3. Experimental results

3.1. Microstructural evolution

SEM micrographs, an EBSD orientation map and the grain size distribution of the alloy after extrusion with an extrusion ratio of 19:1 are shown in Fig. 1. It is apparent from inspection of Figs 1a and b that the microstructure of the alloy consists of fine equiaxed grains indicating the occurrence of dynamic recrystallization (DRX) during extrusion at 673 K. The EBSD orientation map is shown in Fig. 1c and it is clear that fine equiaxed grains are present formed by DRX during deformation. The grain size distribution data in Fig. 1d, obtained from the EBSD analysis, gave an average grain size of $\sim 4.6 \pm 0.2 \mu\text{m}$ for the extruded material. Microstructural and textural evolutions of this alloy in the extruded condition were already described in an earlier report [33]. Similar microstructural information for the material processed by 4 ECAP passes at 623 K is presented in Fig. 2. The SEM micrographs demonstrate that the microstructure is in a

fully-recrystallized state consisting of fine equiaxed grains. The average grain size was estimated by EBSD analysis as $\sim 2.2 \pm 0.2 \mu\text{m}$.

When a thin disk is processed by HPT under an applied pressure, the equivalent von Mises strain, ε , imposed on the disk by torsional straining is given by the relationship [34]

$$\varepsilon = \frac{2\pi Nr}{h\sqrt{3}} \quad (2)$$

where r is the radial distance from the center of the disk and h is the initial thickness of the sample. According to Eq. (2), the strain varies across the disk, as discussed in a recent review [35]. Since the shear punch tests were conducted at a radial distance of $r = 1.5 \text{ mm}$ from the centers of the samples, the equivalent strain was calculated specifically for this radial position and it was recorded as 72.5 after 8 HPT turns.

A TEM micrograph of the alloy at $r \sim 1.5 \text{ mm}$ is shown in Fig. 3 after processing by HPT for 8 turns at room temperature. Equiaxed grains are observed even after this large strain of 72.5 at room temperature. The grain size distribution data, taken from a low magnification image with adequate numbers of grains, show that the average grain size of the alloy in this condition is $\sim 72 \pm 5 \text{ nm}$. This demonstrates conclusively that exceptionally small grain sizes may be attained by introducing very high strains in HPT processing.

3.2. SPT results

To investigate the effects of different microstructures produced by different deformation processes on the superplastic behavior of the material, shear punch tests were conducted at selected test temperatures and strain rates. The SPT curves of the material processed by extrusion, ECAP or HPT are shown in Fig. 4 for a testing temperature of 623 K. Inspection shows that the deformation of the material is strain rate dependent at this temperature and over

the measured strain rates, and this dependency appears to be different for the three processing conditions. At a given temperature, the strain rate sensitivity index value, m , may be obtained from the variation of the shear flow stress, τ , with the strain rate, $\dot{\gamma}$. The method for calculation of the m -value from the SPT data was explained earlier [17,27] and is now summarized briefly.

The high-temperature shear flow stress, τ , is related to the shear strain rate, $\dot{\gamma}$, by a modified power-law relationship of the form [17]

$$\left(\frac{\dot{\gamma}T}{G}\right) = \left(\frac{Ab}{k}\right) \left(\frac{b}{d}\right)^p \left(\frac{\tau}{G}\right)^{\frac{1}{m}} \exp\left(\frac{-Q}{RT}\right) \quad (3)$$

where A is a material parameter, b is the Burgers vector, k is Boltzmann's constant, d is the grain size, p is the inverse grain size exponent, G is the shear modulus, Q is the deformation activation energy, R is the universal gas constant and T is the absolute temperature. To account for the temperature dependence of the shear modulus, G is calculated from the following experimental trend for magnesium [36]:

$$G \text{ (MPa)} = 19200 - 8.6T \text{ (K)} \quad (4)$$

Due to the constancy of Q at a given temperature, it is possible to determine the value of m from the relationship:

$$m = \left(\frac{\partial \ln\left(\frac{\tau}{G}\right)}{\partial \ln\left(\frac{\dot{\gamma}T}{G}\right)}\right)_T \quad (5)$$

Variations of the normalized ultimate shear strength (USS) values (τ_m) of the materials processed by extrusion, ECAP and HPT with the temperature-compensated shear strain rate are shown in Fig. 5 for all test temperatures. As demonstrated by the results, the strain rate sensitivity of the material is temperature dependent for all processing conditions and show relatively large values of about 0.4–0.5 at the optimum deformation temperatures (T_{opt}). Also, the

variations become sigmoidal in shape at these optimum temperatures, demonstrating the operation of different deformation mechanisms in different ranges of shear strain rates and confirming the general characteristics of superplastic materials where optimum tensile elongations are recorded at the highest values of m at which the resistance to necking is greatly enhanced [37]. However, the optimum temperatures are different for the extrusion, ECAP and HPT processes. Specifically, the maximum SRS was obtained at temperatures of 723, 723 and 623 K for the alloy processed by extrusion, ECAP and HPT, respectively. To provide a better representation of the data, the variations of m with the test temperature are shown in Fig. 6 demonstrating a much lower optimum temperature for the HPT process.

In addition to the SRS value, the deformation activation energy maybe calculated from the SPT data at constant shear strain rates. According to Eq. (3), the activation energy is given as

$$Q = \frac{R}{m} \left(\frac{\partial \ln\left(\frac{\dot{\epsilon}}{G}\right)}{\partial \left(\frac{1}{T}\right)} \right) \frac{\dot{\epsilon}T}{G} \quad (6)$$

The normalized USS values of the material are plotted against the reciprocal of temperature at constant temperature-compensated shear strain rates on a semi-logarithmic scale in Fig. 7 for the extrusion, ECAP and HPT processes. These calculations were made in a temperature range of 573–673 K and a temperature compensated shear strain rate $\left(\frac{\dot{\epsilon}T}{G}\right)$ range of 2.0×10^{-3} – 4.0×10^{-3} (K/MPa s) for HPT and in a temperature range of 673–773 K and temperature compensated shear strain rate range of 1.0×10^{-3} – 5.0×10^{-3} and 2.0×10^{-3} – 6.0×10^{-3} (K/MPa s) for the extrusion and ECAP processes, respectively, where this corresponds to the maximum SRS. The average activation energies were determined as $\sim 117 \pm 5$, $\sim 101 \pm 5$, and $\sim 110 \pm 5$ kJ/mol for the extrusion, ECAP and HPT, respectively.

4. Discussion

4.1. Grain refinement by extrusion, ECAP and HPT

Severe plastic deformation processes have been used traditionally to achieve extensive grain refinement of different materials by exerting large amounts of strain. However, different SPD methods produce different efficiencies in the level of grain refinement. In the present research on a GW54 alloy, nano-sized grains with an average size of ~ 72 nm were obtained after 8 turns of HPT, a fine-grained microstructure with average grain size of ~ 2.2 μm was obtained after 4 passes of ECAP and after hot extrusion with an extrusion ratio of 19:1 the average grain size was ~ 4.6 μm . Since the same starting material was used for all experiments, the observed differences in grain size arise only from the different conditions, including the different strains, of the various processing methods.

It has been reported that the grain refinement efficiency is the highest in the primary stages of deformation by SPD and gradually decreases with increasing imposed strain [6]. Also, there exists a saturation strain after which the grain refinement essentially ceases [38,39]. In an earlier investigation of Mg–Gd–Y–Zr alloys, it was found that the saturation strain of these alloys was ~ 4 corresponding to 4 passes of ECAP [24] and about ~ 72 corresponding to 8 turns of HPT [25] and therefore these optimum values were used in the present investigation.

The saturation strain of 4 for ECAP demonstrates that smaller grain sizes cannot be achieved by increasing the numbers of passes. Furthermore, it was not possible to perform ECAP at a temperature lower than 623 K due to the lack of formability [24]. This is a standard problem in the processing of difficult-to-work alloys where ECAP processing is achieved most readily at lower temperatures by increasing the channel angle within the ECAP die [40]. Thus, it appears that the smallest average grain size produced by the ECAP method in the GW54 alloy is ~ 2.2 μm

and it is not generally feasible to achieve nano or ultra-fine grained (UFG) microstructures. On the other hand, semi-hydrostatic deformation may be performed using a high imposed pressure in the HPT processing of Mg alloys [41] so that very large strains may be exerted on these alloys even at room temperature. Accordingly, very small grain sizes in the range of ~100 nm may be attained as a result of the large densities of dislocations introduced in the HPT samples. Therefore, it is concluded for the Mg–Gd–Y–Zr alloys that, although ECAP or even simple extrusion can be used for the production of fine-grained samples, true nano-grained microstructures are most readily produced by HPT and requires a sufficient number of turns to satisfy the saturation strain of ~72. The average grain size of ~72 nm obtained for the GW54 alloy by HPT is one of the smallest grain sizes reported to date for the Mg–Gd alloys, thereby demonstrating the significant capability of HPT processing for the production of nano-grained materials.

4.2. Superplasticity after extrusion, ECAP and HPT

The size of the grains will greatly affect the superplastic behavior of a superplastic material. Accordingly, shear punch tests were used to investigate the superplastic behavior of the Mg–5Gd–4Y–0.4Zr alloy samples with different grain sizes processed through different deformation processes.

The SPT results show that the strain rate sensitivity of the alloy increases with temperature and reaches a maximum at the optimum temperature of superplastic flow and thereafter decreases with further increase in test temperature. The material showed superplastic flow at the optimum test temperatures, with distinct sigmoidal variations of stress with strain rate as anticipated in conventional superplasticity [37] with maximum m -values of ~0.42, ~0.46 and

~0.50 for extrusion, ECAP and HPT, respectively. The optimum temperature of 623 K for the superplastic flow of the material processed by HPT was one hundred degrees lower than the optimum temperature of 723 K for the extrusion and ECAP processes. The reason is because superplastic flow is associated with the occurrence of grain boundary sliding (GBS) [42] and this requires the diffusion and redistribution of alloying elements during high temperature deformation. However, because of the low diffusion rates of Gd and Y in the Mg matrix [43,44], low deformation temperatures are not suitable for superplastic deformation in the Mg–Gd–Y alloys. Therefore, the fine-grained material produced by extrusion and ECAP failed to show superplastic flow at temperatures lower than 723 K. Similar results have been reported for other fine-grained Mg–Gd base alloys [13,15,45]. On the other hand, by decreasing the grain size to the nano scale of <100 nm, the diffusional processes are assisted due to the increased fraction of grain boundaries. Accordingly, the nano-grained GW54 alloy exhibited optimum superplasticity at 623 K. The observed decrease in the values of the strain rate sensitivity after the optimum temperatures is related to grain growth as discussed in earlier reports on Mg–Gd–Y–Zr alloys [17,24,25].

The dominant deformation mechanism for the material in the superplastic region may be evaluated using the activation energy and strain rate sensitivity values obtained from the SPT results. The material showed m -values of ~0.4–0.5 at the optimum temperatures for superplastic flow (623 K for HPT and 723 K for extrusion and ECAP), which is in accordance with the SRS of ~0.5 associated with GBS [42]. The activation energy of the material processed by HPT was ~110±5 kJ/mol in the temperature range of 573–673 K. Activation energies of ~117± 5 and ~101 ± 5 kJ/mol were also obtained for the material processed by extrusion and ECAP, respectively, where these values were calculated in the temperature range of 673–773 K. These activation

energies are also generally close to the activation energy for grain boundary diffusion in Mg (~92 kJ/mol [46]). Therefore, both the SRS values and activation energies suggest that GBS controlled by grain boundary diffusion is the dominant deformation mechanism in the GW54 alloy in the optimum ranges of strain rate and temperature for superplastic flow after processing by extrusion, ECAP and HPT. This mechanism is consistent with the fine-grained and nano-grained microstructures of the alloy and the sigmoidal dependence of the SRS on the shear strain rate at the optimum temperatures, as well as with recent analyses showing that superplastic flow in magnesium-based alloys processed by either ECAP or HPT follows the conventional theoretical model for grain boundary sliding [47-49].

5. Conclusions

Comparison of the microstructure and superplasticity of an Mg–5Gd–4Y–0.4Zr alloy processed by equal-channel angular pressing and high-pressure torsion yielded the following conclusions:

1. An Mg–5Gd–4Y–0.4Zr alloy was investigated to determine the effect on grain refinement and superplastic properties when using the three different processing procedures of extrusion, ECAP or HPT. HPT was conducted at room temperature to the relatively large strain of ~72.5 but it was not possible to process the alloy at temperatures lower than 673 and 623 K in the extrusion and ECAP processes
2. Average grain sizes of $\sim 4.6 \pm 0.2$ and 2.2 ± 0.2 μm were obtained in extrusion and after 4 passes of ECAP but the grain size was much reduced to $\sim 72 \pm 10$ nm after 8 turns of HPT.

3. Shear punch results gave strain rate sensitivity values of $\sim 0.42 \pm 0.05$, $\sim 0.46 \pm 0.05$ and $\sim 0.50 \pm 0.05$ for the extrusion, ECAP and HPT processes, respectively. The optimum temperature for superplastic flow was 623 K for HPT and 723 K for extrusion and ECAP. The activation energies were $\sim 117 \pm 5$, $\sim 101 \pm 5$ and $\sim 110 \pm 5$ kJ/mol after extrusion, ECAP and HPT, respectively. The results are consistent with grain boundary sliding as the dominant deformation mechanism in the superplastic region.

4. The results show HPT is the optimum processing route for grain refinement and superplasticity of the GW54 alloy by comparison with extrusion and ECAP. The main advantage of HPT is the capability of processing at room temperature and thereby exerting a high imposed strain without cracking. This leads to exceptional grain refinement and a lower temperature for superplastic flow.

Acknowledgments

The authors thank the Iran National Science Foundation (INSF) for support of this work under Grant no. 94013486. Three of the authors were supported by the European Research Council under ERC Grant Agreement No. 267464-SPDMETALS (PHRP, YH, TGL).

References

- [1] B.L. Mordike, T. Ebert, Magnesium: properties–applications–potential, *Mater. Sci. Eng. A* 302 (2001) 37–45.
- [2] H. Watanabe, T. Mukai, M. Kohzu, S. Tanabe, K. Higashi, Effect of temperature and grain size on the dominant diffusion process for superplastic flow in an AZ61 magnesium alloy, *Acta Mater.* 47 (1999) 3753–3758.
- [3] Y.H. Wei, Q.D. Wang, Y.P. Zhu, H.T. Zhou, W.J. Ding, Y. Chino, M. Mabuchi, Superplasticity and grain boundary sliding in rolled AZ91 magnesium alloy at high strain rates, *Mater. Sci. Eng. A* 360 (2003) 107–115.
- [4] L. Lin, W. Wu, L. Yang, L. Chen, Z. Liu, Grain boundary sliding and accommodation mechanisms during superplastic deformation of ZK40 alloy processed by ECAP, *J. Mater. Sci.* 41(2006) 409–415.
- [5] A.J. Barnes, Superplastic forming: 40 years and still growing, *J. Mater. Eng. Perform.* 16 (2007) 440–454.
- [6] Y. Xun, F.A. Mohamed, Refining efficiency and capability of top-down synthesis of nanocrystalline materials, *Mater. Sci. Eng. A* 528 (2011) 5446–5452.
- [7] Y.Z. Tian, S.D. Wu, Z.F. Zhang, R.B. Figueiredo, N. Gao, T.G. Langdon, Comparison of microstructures and mechanical properties of a Cu–Ag alloy processed using different severe plastic deformation modes, *Mater. Sci. Eng. A* 528 (2011) 4331–4336.
- [8] S. Sabbaghianrad, T.G. Langdon, A critical evaluation of the processing of an aluminum 7075 alloy using a combination of ECAP and HPT, *Mater. Sci. Eng. A* 596 (2014) 52–58.
- [9] J. Wongsan-Ngam, H. Wen, T.G. Langdon, Microstructural evolution in a Cu–Zr alloy processed by a combination of ECAP and HPT, *Mater. Sci. Eng. A* 579 (2013) 126–135.
- [10] A.P. Zhilyaev, S. Lee, G.V. Nurislamova, R.Z. Valiev, T.G. Langdon, Microhardness and microstructural evolution in pure nickel during high-pressure torsion, *Scr. Mater.* 44 (2001) 2753–2758.
- [11] A.P. Zhilyaev, G.V. Nurislamova, B.K. Kim, M.D. Baró, J.A. Szpunar, T.G. Langdon, Experimental parameters influencing grain refinement and microstructural evolution during high-pressure torsion, *Acta Mater.* 51 (2003) 753–765.

- [12] J. Wongsan-Ngam, M. Kawasaki, T.G. Langdon, A comparison of microstructures and mechanical properties in a Cu-Zr alloy processed using different SPD techniques, *J. Mater. Sci.* 48 (2013) 4653–4660.
- [13] J. Čížek, I. Procházka, B. Smola, I. Stuliková, R. Kužel, Z. Matěj, V. Cherkaska, R.K. Islamgaliev, O. Kulyasova, Microstructure and thermal stability of ultra fine grained Mg-based alloys prepared by high-pressure torsion, *Mater. Sci. Eng. A* 462 (2007) 121–126.
- [14] R. Alizadeh, R. Mahmudi, A.H.W. Ngan, T.G. Langdon, Microstructural stability and grain growth kinetics in an extruded fine-grained Mg–Gd–Y–Zr alloy, *J. Mater. Sci.* 50 (2015) 4940–4951.
- [15] X. Zhang, L. Li, Y. Deng, N. Zhou, Superplasticity and microstructure in Mg–Gd–Y–Zr alloy prepared by extrusion, *J. Alloys Compd.* 481 (2009) 296–300.
- [16] D.J. Li, Q.D. Wang, J.J. Blandin, M. Suery, J. Dong, X.Q. Zeng, High temperature compressive deformation behavior of an extruded Mg–8Gd–3Y–0.5Zr (wt.%) alloy, *Mater. Sci. Eng. A* 526 (2009) 150–155.
- [17] R. Alizadeh, R. Mahmudi, T.G. Langdon, Superplasticity of a fine-grained Mg–9Gd–4Y–0.4Zr alloy evaluated using shear punch testing, *J. Mater. Res. Technol.* 3 (2014) 228–232.
- [18] A. Movahedi-Rad, R. Mahmudi, G.H. Wu, H.R. Jafari Nodooshan, Enhanced superplasticity in an extruded high strength Mg–Gd–Y–Zr alloy with Ag addition, *J. Alloys Compd.* 626 (2015) 309–313.
- [19] Q. Yang, B.L. Xiao, Z.Y. Ma, Enhanced superplasticity in friction stir processed Mg–Gd–Y–Zr alloy, *J. Alloys Compd.* 551 (2013) 61–66.
- [20] Q. Yang, B.L. Xiao, Q. Zhang, M.Y. Zheng, Z.Y. Ma, Exceptional high-strain-rate superplasticity in Mg–Gd–Y–Zn–Zr alloy with long-period stacking ordered phase, *Scr. Mater.* 69 (2013) 801–804.
- [21] L. Li, X. Zhang, Y. Deng, C. Tang, Superplasticity and microstructure in Mg–Gd–Y–Zr rolled sheet, *J. Alloys Compd.* 485 (2009) 295–299.
- [22] L. Li, X. Zhang, C. Tang, Y. Deng, N. Zhou, Mechanical properties and deep draw ability of Mg–Gd–Y–Zr alloy rolling sheet at elevated temperatures, *Mater. Sci. Eng. A* 527 (2010) 1266–1274.

- [23] M. Sarebanzadeh, R. Roumina, R. Mahmudi, G.H. Wu, H.R. Jafari Nodooshan, Enhancement of superplasticity in a fine-grained Mg–3Gd–1Zn alloy processed by equal-channel angular pressing, *Mater. Sci. Eng. A* 646 (2015) 249–253.
- [24] R. Alizadeh, R. Mahmudi, A.H.W. Ngan, P.H.R. Pereira, Y. Huang, T.G. Langdon, Microstructure, texture and superplasticity of a fine-grained Mg–Gd–Zr alloy processed by equal-channel angular pressing, *Metall. Mater. Trans.* 47A (2016) 6056–6069.
- [25] R. Alizadeh, R. Mahmudi, A.H.W. Ngan, Y. Huang, T.G. Langdon, Superplasticity of a nano-grained Mg–Gd–Y–Zr alloy processed by high-pressure torsion, *Mater. Sci. Eng. A* 651(2016)786–794.
- [26] G.L. Hankin, M.B. Toloczko, M.L. Hamilton, R.G. Faulkner, Validation of the shear punch-tensile correlation technique using irradiated materials, *J. Nucl. Mater.* 258–263 (1998) 1651–1656.
- [27] R. Mahmudi, R. Alizadeh, Sh. Azhari, Strain rate sensitivity of equal-channel angularly pressed Sn–5Sb alloy determined by shear punch test, *Mater. Lett.* 97 (2013) 44–46.
- [28] R.B. Figueiredo, P.R. Cetlin, T.G. Langdon, Using finite element modeling to examine the flow processes in quasi-constrained high-pressure torsion, *Mater. Sci. Eng. A* 528 (2011) 8198–8204.
- [29] M. Furukawa, Y. Iwahashi, Z. Horita, M. Nemoto, T.G. Langdon, The shearing characteristics associated with equal-channel angular pressing, *Mater. Sci. Eng. A* 257 (1998) 328–332.
- [30] Y. Iwahashi, J. Wang, Z. Horita, M. Nemoto, T.G. Langdon, Principle of equal-channel angular pressing for the processing of ultrafine-grained materials, *Scr. Mater.* 35 (1996) 143–146.
- [31] R. Alizadeh, R. Mahmudi, Evaluating high-temperature mechanical behavior of cast Mg–4Zn–xSb magnesium alloys by shear punch testing, *Mater. Sci. Eng. A* 527 (2010) 3975–3983.
- [32] R.K. Guduru, K.A. Darling, R. Kishore, R.O. Scattergood, C.C. Koch, K.L. Murty, Evaluation of mechanical properties using shear–punch testing, *Mater SciEng A* 395 (2005) 307–314.
- [33] R. Alizadeh, R. Mahmudi, A.H.W. Ngan, T.G. Langdon, An unusual extrusion texture in Mg–Gd–Y–Zr alloys, *Adv. Eng. Mater.*, 18 (2016) 1044–1049.

- [34] R.Z. Valiev, Yu.V. Ivanisenko, E.F. Rauch, B. Baudelet, Structure and deformation behaviour of Armco iron subjected to severe plastic deformation, *Acta Mater.* 44 (1996) 4705–4712.
- [35] A.P. Zhilyaev, T.G. Langdon, Using high-pressure torsion for metal processing: Fundamentals and applications, *Prog. Mater. Sci.* 53 (2008) 893–979.
- [36] S.S. Vagarali, T.G. Langdon, Deformation mechanisms in h.c.p. metals at elevated temperatures—I. Creep behavior of magnesium, *Acta. Met.* 29 (1981) 1969–1982.
- [37] H. Ishikawa, F.A. Mohamed, T.G. Langdon, The influence of strain rate on ductility in the superplastic Zn-22% Al eutectoid, *Phil. Mag.* 32 (1975) 1269-1271.
- [38] R. Pippan, F. Wetscher, M. Hafok, A. Vorhauer, I. Sabirov, The limits of refinement by severe plastic deformation, *Adv. Eng. Mater.* 8 (2006) 1046-1056.
- [39] R. Pippan, S. Scheriau, A. Taylor, M. Hafok, A. Hohenwarter, A. Bachmaier, Saturation of fragmentation during severe plastic deformation, *Ann. Rev. Mater. Res.* 40 (2010) 319-343.
- [40] R.B. Figueiredo, P.R. Cetlin, T.G. Langdon, The processing of difficult-to-work alloys by ECAP with an emphasis on magnesium alloys, *Acta Mater.* 55 (2007) 4769–4779.
- [41] Y. Huang, R.B. Figueiredo, T. Baudin, F. Brisset, T.G. Langdon, Evolution of strength and homogeneity in a magnesium AZ31 alloy processed by high-pressure torsion at different temperatures, *Adv. Eng. Mater.* 14 (2012) 1018–1026.
- [42] T.G. Langdon, A unified approach to grain boundary sliding in creep and superplasticity, *Acta Metall. Mater.* 42 (1994) 2437–2443.
- [43] S.K. Das, Y.M. Kim, T.K. Ha, R. Gauvin, I.H. Jung, Anisotropic diffusion behavior of Al in Mg: Diffusion couple study using Mg single crystal, *Metall. Mater. Trans. A* 44 (2013) 2539–2547.
- [44] S.K. Das, Y.B. Kang, T. Ha, I.H. Jung, Thermodynamic modeling and diffusion kinetic experiments of binary Mg–Gd and Mg–Y systems, *Acta Mater.* 71 (2014) 164–175.
- [45] L. Li, X. Zhang, C. Tang, Y. Deng and N. Zhou, Mechanical properties and deep drawability of Mg–Gd–Y–Zr alloy rolling sheet at elevated temperatures, *Mater. Sci. Eng. A* 527(2010) 1266–1274.
- [46] H.J. Frost, M.F. Ashby, *Deformation-Mechanism Maps: The Plasticity and Creep of Metals and Ceramics*, Pergamon Press, Oxford, U.K. (1982).

- [47] M. Kawasaki, T.G. Langdon, Principles of superplasticity in ultrafine-grained materials, *J. Mater. Sci.* 42 (2007) 1782-1796.
- [48] M. Kawasaki, T.G. Langdon, Review: achieving superplasticity in metals processed by high-pressure torsion, *J. Mater. Sci.* 49 (2014) 6487–6496.
- [49] M. Kawasaki, T.G. Langdon, Review: achieving superplasticity in ultrafine-grained materials at high temperatures, *J. Mater. Sci.* 15 (2016) 19-32.

Accepted manuscript

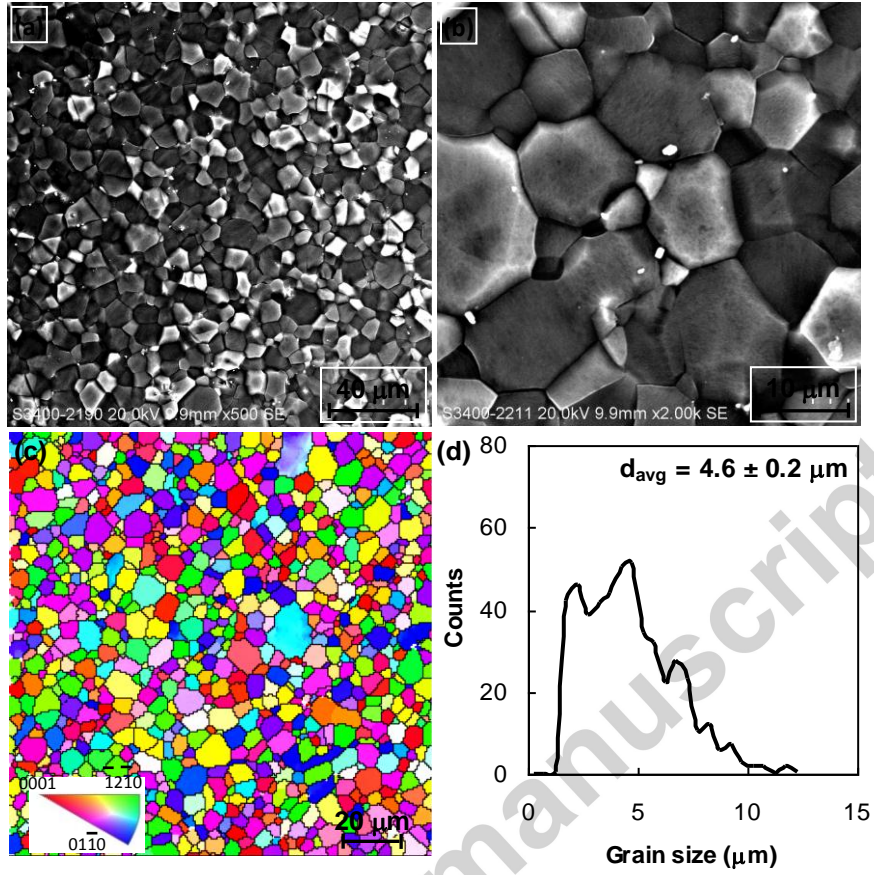


Fig. 1. (a) and (b) SEM micrographs, (c) EBSD orientation map, and (d) grain size distribution of the alloy after extrusion.

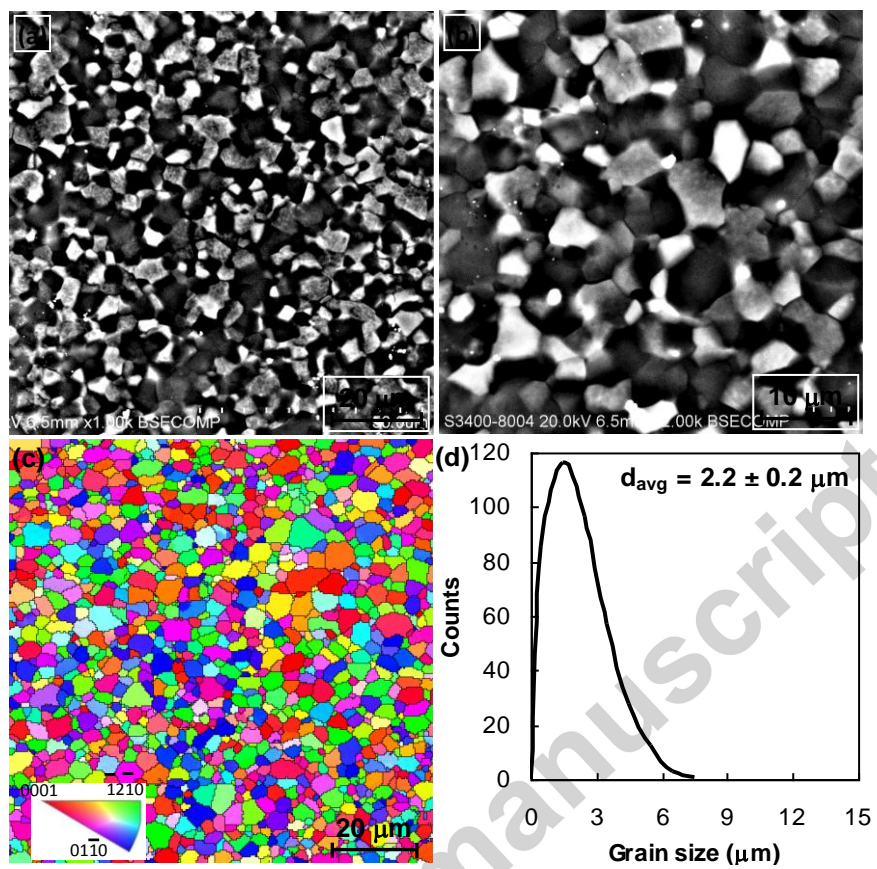


Fig. 2. (a) and (b) SEM micrographs, (c) EBSD orientation map, and (d) grain size distribution of the alloy after 4 ECAP passes.

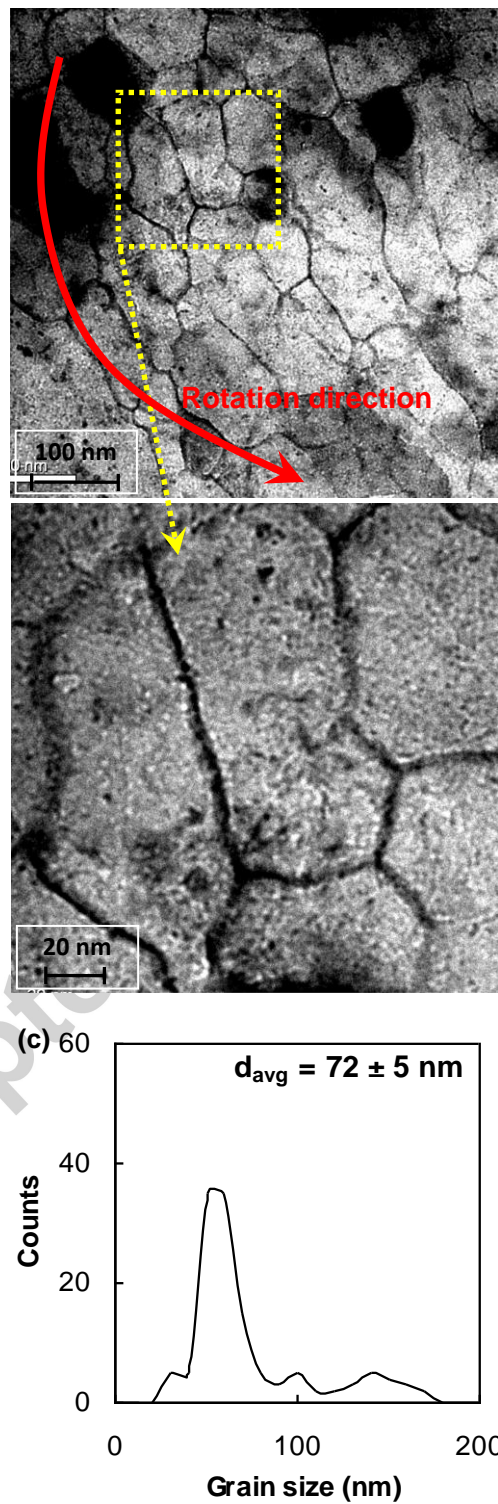


Fig. 3. TEM micrographs (a,b), and grain size distribution of the alloy (c) after 8 HPT turns.

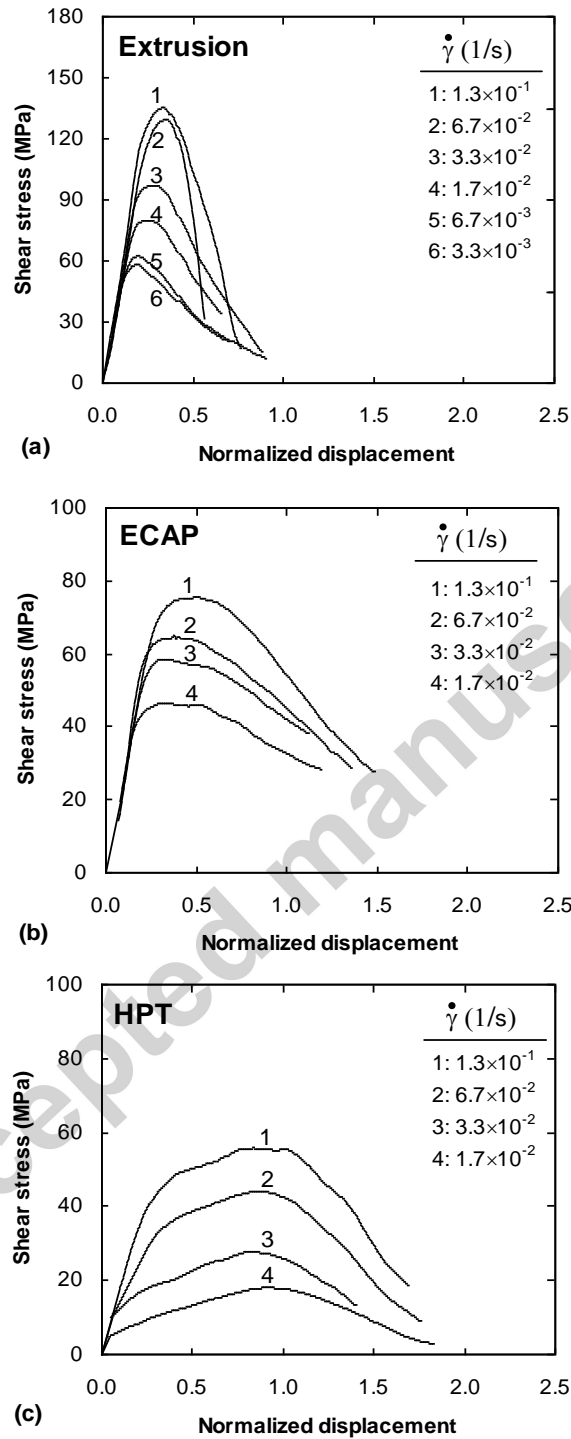


Fig. 4. SPT curves of the material, processed by extrusion (a), ECAP (b) and HPT (c), at 623 K and at different strain rates.

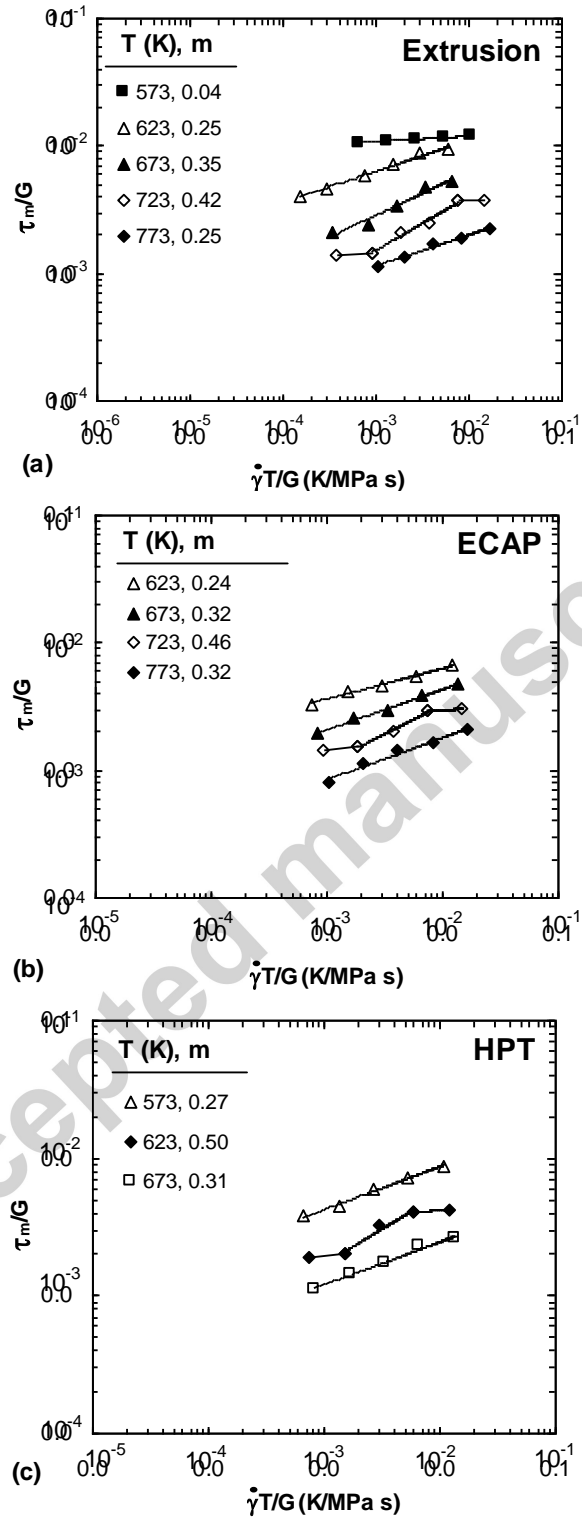


Fig. 5. Normalized τ_m of the material, processed by extrusion (a), ECAP (b) and HPT (c), as a function of temperature-compensated shear strain rate at different temperatures.

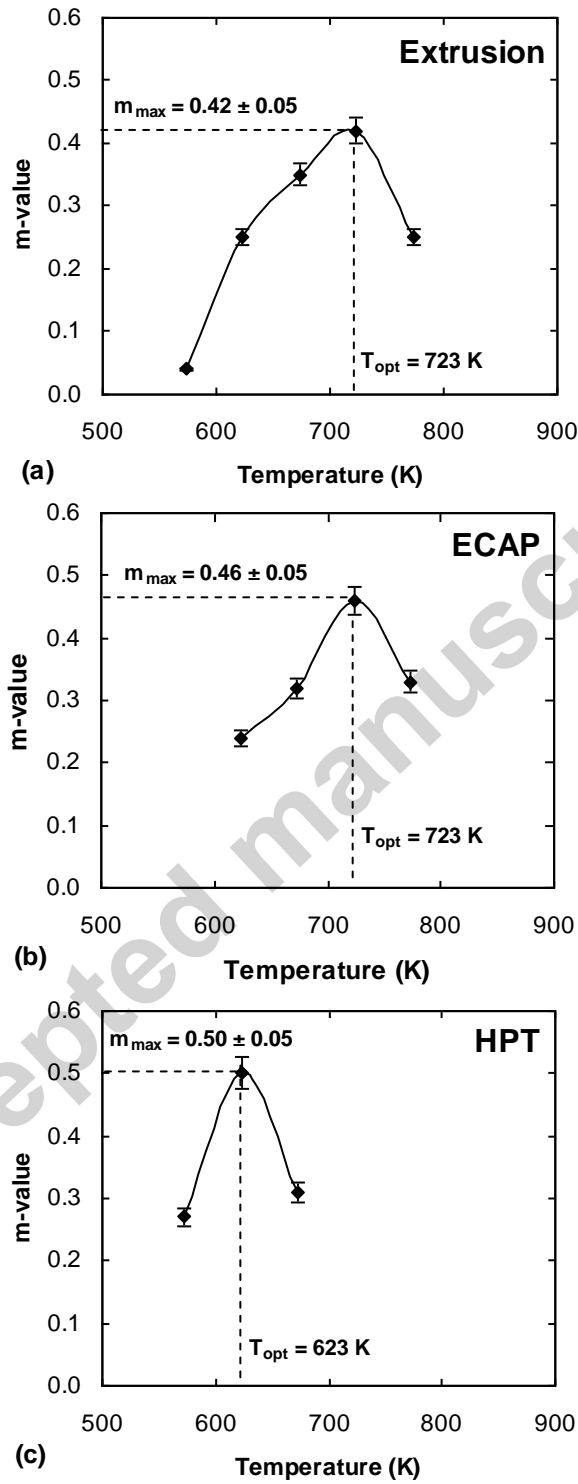


Fig. 6. Variations of m -value with test temperature, for the material processed by extrusion (a), ECAP (b) and HPT (c).

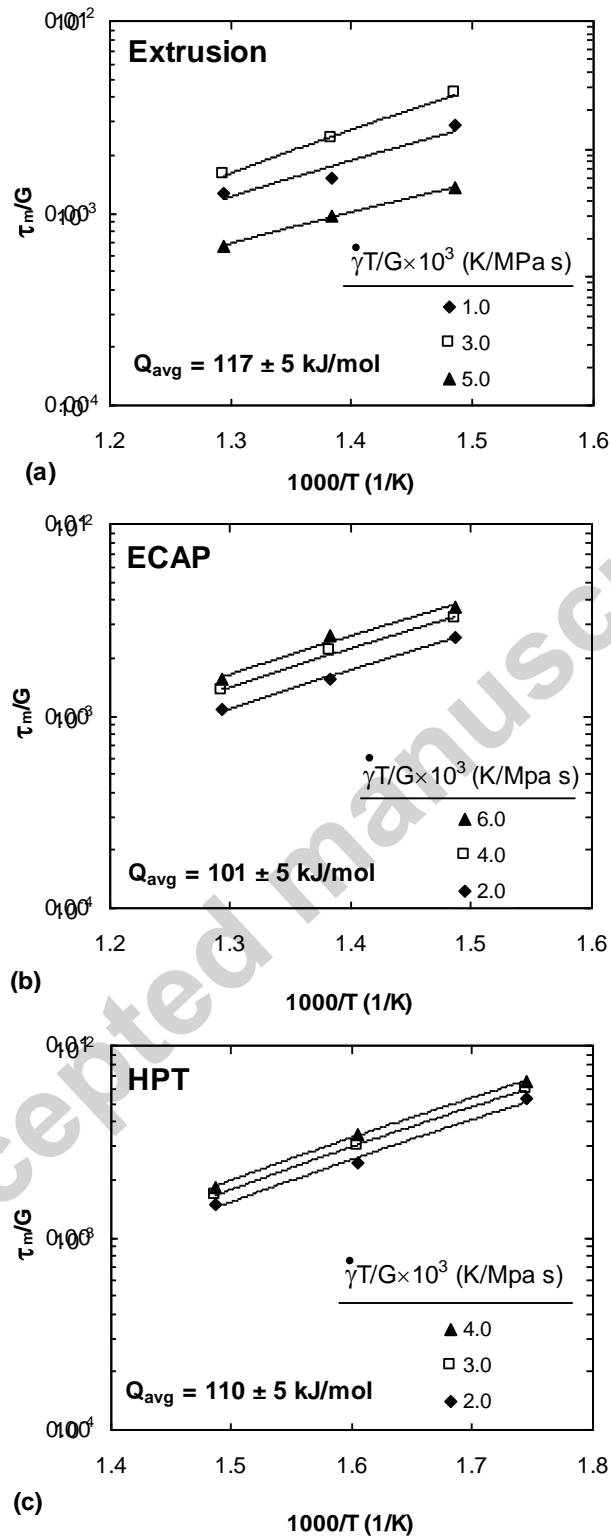


Fig. 7. Temperature dependence of normalized τ_m values at constant temperature-compensated shear strain rates for the alloy after processing by extrusion (a), ECAP (b) and HPT (c).

Table 1. Summary of the grain size data for some alloys processed by ECAP and HPT

Alloys or compositions (wt%)	SPD			Grain size (nm)	Reference
	Process	Temperature (K)	Number of passes or turns		
Cu-8Ag	ECAP	RT	8	109	Tian <i>et al.</i> [7]
	HPT	RT	5	40	
Al-7075 ¹	ECAP	473	4	680	Sabbaghianrad <i>et al.</i> [8]
	HPT ²	RT	20	310	
Cu-0.1Zr	ECAP	RT	8	310	Wongsa-Ngam <i>et al.</i> [9]
	HPT ³	RT	5	270 ⁴	

¹Al-7075: Al-5.6Zn-2.5Mg-1.6Cu.

²HPT was conducted after processing samples by 4 ECAP passes at 473 K.

³HPT was conducted after processing samples by 8 ECAP passes at 473 K.

⁴The grain size was measured at the edge of the HPT discs.